Journal of Electrical Engineering, Vol. 75, No. 5, 2024, pp. 411-417

sciendo
PAPERS

Compact log-periodic microstrip DGS filters with high figure-of-merit

Jia-Lin Li [1], Baidenger Agyekum Twumasi [1, 2], Rong-Bin Chen [3], Shan-Shan Gao [4]

This contribution is an extended in-depth study of our previously initial research work about the compact Log-periodic microstrip DGS lowpass filters. The improved filters proposed use a log-periodic zig-zag structure defected on the ground plane under a compensated microstrip line for microwave filter applications. More importantly, a comprehensive index called figure-of-merit (FoM) is introduced in this paper to characterize the achieved performance of this kind of filters. Results show that high FoMs can be realized for this contribution. The developed filters B and C have dimensions 30.307 mm × 31.17 mm and 22.35 mm × 31.524 mm, while the achieved FoMs for the two demonstrators are approximately 3.5×10^4 and 3.1×10^4, respectively.

Keywords: microwave filter, log-periodic, defected ground structure (DGS), suppression band, figure-of-merit (FoM)

1 Introduction

Microwave filters can be used to separate or combine different frequency channels for microwave engineering applications. They are indispensable in many RF/microwave systems. This has been demonstrated by the recent increase in various filter studies ranging from lowpass filters (LPFs) to bandstop filters [1, 2]. The introduction of geometrical patterns etched off on the back-side metallic ground plane of microstrip-based filter designs has shown attractive results in application to the microwave and RF domains [3, 4]. These etched shapes can manipulate the frequency responses, yielding a class of microwave filters referred to as defected ground structure (DGS) filters. The DGS can reject frequency bands because of the slow-wave effect that leads to increasing the effective inductance and capacitance of the microwave transmission line. This design technique is a good choice to achieve low-profile compact filters without compromising on the electric performance.

In [4], authors presented a flexible microstrip LPF fabricated on a polyimide film substrate. The proposed filter consists of ten cascaded asymmetrical Pi-shaped DGS resonators. This filter has a low insertion loss of less than 1.9 dB under the cut-off frequency of 2.2 GHz, and a wide stopband from 2.7 to 12 GHz with a rejection level over 50 dB. It is characterized by a sharp transition band, an ultra-wide stopband with a high rejection level compared with previously reported microstrip LPFs with symmetrical or asymmetrical DGSs. In [5], a hairpin DGS LPF with a simple architecture that can present attenuation and reflection poles near the cut-off frequency was reported, where a wide stopband with a high suppression level was demonstrated. In [6], a five-stage dumbbell-shaped DGS was developed for microwave differential bandpass filter applications, where the presented equivalent lumped LC model predicated the in-band response well. In [7], log-periodic zig-zag DGS with simple architecture was studied for wide suppression band LPF applications.

On the other hand, small estate-size and high-performance LPFs having wide stopband, good return loss and low insertion loss are in high demand for RF/microwave engineering. This is due to the ability of such filters to inhibit wideband noise and spurious signals which is important in wireless systems [8, 9]. In [8], asymmetric Koch fractal Pi-shaped DGS LPFs with single and two cascaded resonators were presented. The reported LPFs have wide stopbands and sharp transition bands. For a single unit cell, it can achieve a passband up to 1.9 GHz with an insertion loss of less than 0.5 dB, and a stopband from 2 GHz to 8 GHz with an attenuation level over 12 dB. In [10], the authors' simulation studied a compact ultra-wideband filter having a wide stopband using a modified multi-mode resonator-based structure in combination with DGS based LPF configuration. With meandering high impedance line loading to a strip to form the defected ground, the study reported in [11] shows that a wide stopband LPF can be developed by further using stub loading and spur line on the microstrip line. In general, microwave filters with simple architecture without compromising stringent requirements are much desired in modern RF/microwave systems.

[1] School of Resources and Environment, University of Electronic Science and Technology of China (UESTC), Chengdu 611731, China
[2] Department of Electrical/Electronic Engineering, Ho Technical University, Ho, Ghana
[3] Department of Electronic and Information Technology, Jiangmen Polytechnic, Jiangmen 529030, China
[4] School of Electronic Information and Electrical Engineering, Chengdu University, Chengdu 610106, China
S.-S. Gao, ssgao@cdu.edu.cn

https://doi.org/10.2478/jee-2024-0049, Print (till 2015) ISSN 1335-3632, On-line ISSN 1339-309X

Based on our previous study, the log-periodic zig-zag based DGS is further discussed in detail in this paper. The developed filters feature a wide stopband and low insertion loss within the passband as well as a sharp transition between the passband and stopband. To effectively characterize the achieved performance of such kinds of filters, a comprehensive index called figure-of-merit (FoM) is studied in this work. Prototype filters are developed, fabricated, and demonstrated. Simulation and measurement results are presented and compared. They show good agreement and hence, high FoMs can be achieved for the proposed filters.

2 Analyses on the slotline base DGS

The log-periodic zig-zag DGS is based on the slotline, the same as studied in [7]. The idea arose from the principle of log-periodic antenna design. It is known that the log-periodic antenna is a frequency-independent antenna composed of resonant elements. Here the slots are etched on the ground plane of a microwave substrate under a compensated microstrip line. The substrate used has a relative permittivity of ε_r=9.6 and a thickness of h=0.8mm.

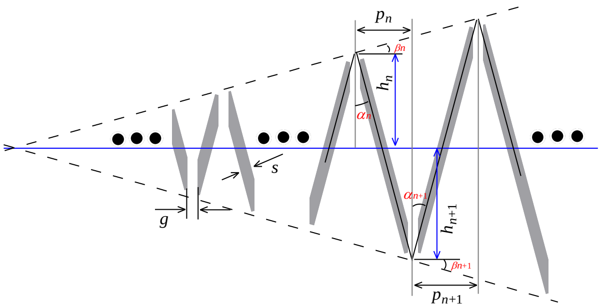

Fig. 1. The studied log-periodic zig-zag DGS etched on the ground plane

For the general case of the log-periodic antenna, the resonant elements are parallel to each other but for the proposed log-periodic DGS structure the resonant elements were etched on the ground plane and have been arranged in a zig-zag fashion (slanted resonant elements) with a small gap of ‘g’ between the tip of each vertex of the zig-zag resonant elements, as shown in Fig. 1 and the same as in our previous study in [7].

Also, referred to the horizontal axis shown in Fig. 1 (corresponding to the central line, which is also the direction of the positioned microstrip line), the height from the vertex of each zig-zag to the central line is h_n, for the n^{th} slanted slot. Similarly, it is marked as h_{n+1} for the $(n+1)^{\text{th}}$ slot. The spacing between two adjacent apexes is p_n related to the n^{th} slot. The two parameters are called geometric ratio or scale factor which can be given by the height ratio described in (1),

$$h_{n+1}=\frac{h_n}{\tau_h}=\cdots=\frac{h_1}{\tau_h^n} \tag{1}$$

for the spacing ratio,

$$p_{n+1}=\frac{p_n}{\tau_p}=\cdots=\frac{p_1}{\tau_p^n}. \tag{2}$$

Here, both ratios of τ_h and τ_p are less than 1. To separate the slots between two adjacent apexes of the zig-zag, a small gap that is denoted as ‘g’ is introduced at the tip of each apex as shown in Fig. 1.

The height h_n and spacing p_n co-determine the length of the related slot and further determine its resonance. On the other hand, the zig-zag fashion also leads to a half vertex angle α_n and a horizontal angle β_n related to the n^{th} slanted slot and so are the α_{n+1} and β_{n+1} for the adjacent $(n+1)^{\text{th}}$ slot. Different from the previous study in [7], we will detail these parameters here. Referring to Fig. 1, it is observed that for the n^{th} slot

$$\tan\alpha_n=\frac{\tau_p}{1+\tau_h}\left(\frac{\tau_h}{\tau_p}\right)^n\frac{p_1}{h_1} \tag{3}$$

and

$$\tan\beta_n=\frac{1-\tau_h^2}{(1+\tau_p)\tau_h}\left(\frac{\tau_p}{\tau_h}\right)^n\frac{h_1}{p_1}, \tag{4}$$

while for the $(n+1)^{\text{th}}$ slot

$$\tan\alpha_{n+1}=\frac{\tau_p}{1+\tau_h}\left(\frac{\tau_h}{\tau_p}\right)^{n+1}\frac{p_1}{h_1} \tag{5}$$

and

$$\tan\beta_{n+1}=\frac{1-\tau_h^2}{(1+\tau_p)\tau_h}\left(\frac{\tau_p}{\tau_h}\right)^{n+1}\frac{h_1}{p_1}. \tag{6}$$

All these result in

$$\frac{1-\tau_h}{1+\tau_p}\cdot\frac{\tau_p}{\tau_h}=\tan\alpha_n\tan\beta_n=\tan\alpha_{n+1}\tan\beta_{n+1}. \tag{7}$$

To this end, Eqn. (7) presents the relationship between the vertex angles α_n and horizontal angles β_n as well as the ratios of τ_h and τ_p. Now, if one sets the height ratio and the spacing ratio to be $\tau_h=\tau_p=\tau$, the above results will become

$$\cdots=\alpha_n=\alpha_{n+1}=\cdots=\alpha \tag{8}$$

for all vertex angles of the slot array and

$$\cdots=\beta_n=\beta_{n+1}=\cdots=\beta \tag{9}$$

for all horizontal angles of the slot array while

$$\tau=\frac{1-\tan\alpha\tan\beta}{1+\tan\alpha\tan\beta} \tag{10}$$

On the other hand, if we set $\alpha=\beta$, Eqn. (7) would lead to

$$\alpha = \beta = \tan^{-1}\sqrt{\frac{1-\tau_h}{1+\tau_p}\cdot\frac{\tau_p}{\tau_h}}\,. \tag{11}$$

If one sets both $\tau_h=\tau_p=\tau$ and $\alpha=\beta$, Eqn. (7) would become a very simple style as given by

$$\tau = \cos 2\alpha = \cos 2\beta\,. \tag{12}$$

In practice, both angles of α and β are in the range of 0 to 90 degrees, so τ is less than one as described earlier. Based on the above discussions, the geometric parameters of this kind of DGS can be determined and so is the filter design as presented below.

3 Developing microstrip lowpass filters based on the studied DGS

The above discussions are further explored for application to the DGS filter designs. Here we first examine the previous studies presented in [7]. Based on the optimal scheme using full-wave electromagnetic (EM) numerical simulations, the final parameters are given by h_{10}=16 mm with τ (=τ_p=τ_h)=0.835, leading to p_1=1.999 mm and h_1=3.164 mm. Correspondingly, the angles are α=16° and β=17.38° from the layout measurements, while the results from Eqns. (3) and (4) are α=16.04° and β=17.37°, showing good agreements. The filter has a measured 3 dB cut-off frequency of 1.96 GHz and a layout footprint of 40.653×29.546 mm^2. We marked this filter as prototype Filter A for reference.

3.1 Prototype filter B: Compact footprint and wide stopband design

Now, we are devoting to the compact design, except for the wide suppression band, for this kind of filters. Also, for simplicity, the ratios are set as τ_p=τ_h=τ, and referring to Filter A, it is approximately 0.85. To achieve compactness, the longitudinal dimension should be compressed, corresponding to reducing the periodicity length p_i. On the other hand, to maintain the same suppression band, the height dimension should be enlarged because of the decreased p_i to hold a similar resonance. Thus, the corresponding height h_i is increased here. To this end, we directly set the first periodicity length and the height as p_1=1.6 mm and h_1=3.8 mm, referring to the result of Filter A, to maintain similar resonance.

After optimal search using EM simulations, the ratio τ is found to be 0.8479. It is noted that in this process, the compensated microstrip line is utilized and it is co-optimized with the ratio parameter τ. Results show the optimized characteristic impedance for the compensated microstrip line is 33.35 Ω. The layout shows a half vertex angle of α=10.93° with a horizontal angle of β=23.08°, as compared with the calculations from Eqns. (3) and (4) being α=10.93° and β=23.07°. The layout indicates that the filter has a footprint of 30.307×31.170 mm^2, meaning the longitude is reduced with a slightly increased lateral size, thus a decreased footprint as compared to the prototype Filter A. Figure 2 shows the layout of this filter, also having 9 slots under a compensated microstrip line.

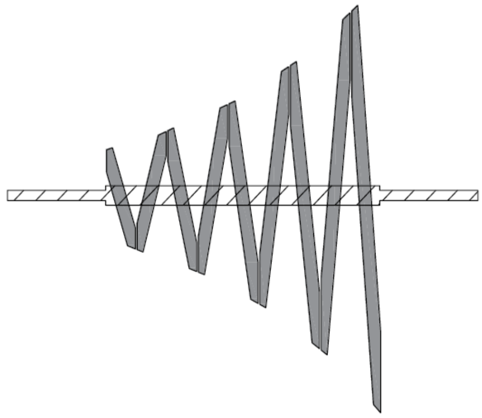

Fig. 2. Layout of the studied zig-zag prototype Filter B, where the grey is the slotline DGS on the metal ground plane, the slanting shadow is the strip on the front side, and the substrate is not shown here for simplicity.

3.2 Prototype filter C: Flexible design with high figure-of-merit

Studies show that the longitude can achieve a minimum when a maximum horizontal periodicity ratio τ_p occurs, that is to say, τ_p approaches 1. Hence for this demonstration, we set the initial parameters as τ_p=1, τ_h=0.85, h_1=3.8 mm, and p=2.5 mm for all periodicity dimensions as a result of τ_p=1. Notice that only parameter τ_h is searched in the optimal process for time-efficiency considerations, while the characteristic impedance of the compensation line is also 33.35 Ω in this design. An optimal value of τ_h=0.8349 is determined after full-wave EM numerical calculations.

Results show that the layout has an exponential contour along the longitude because of a fixed τ_p of 1. By curve-fitting the data of vertexes, one can find a trajectory expression given by

$$y = 3.8e^{0.07x}\,. \tag{13}$$

Shown in Fig. 3 is the filter layout of this flexible design that has a footprint of 22.35 × 31.524 mm^2. It is seen that each slot has different vertex and horizontal angles α_n and β_n that can be evaluated from Eqns. (3) and (4). Owing to the increased height h_n under a fixed longitudinal periodicity dimension p, the vertex angle α_n would keep reducing and go smaller and smaller but on the contrary, the horizontal angle β_n could keep increasing (becoming larger) as the slot number increases. In this design, 9 slots are selected for comparison purposes referring to the prototype Filters A and B.

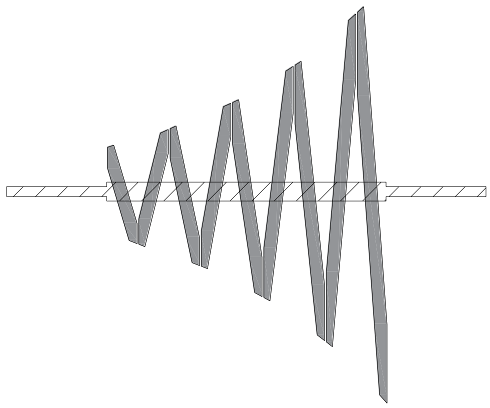

Fig. 3. Layout of the prototype Filter C with maximized horizontal periodicity ratio τ_p=1, where exponential contour along the longitude is found.

4 Experimental demonstrations and discussions on the prototype filters B and C

The optimally developed Filters B and C are further built for performance demonstrations. Figure 4 shows the photographs of the fabricated demonstrators. For filter B, Fig. 5 shows the measured and simulated S parame-ters. Measurements indicate that the 3 dB cutoff frequency is shifted to 1.965 GHz as compared with the simulated one for 2.04 GHz. The in-band insertion loss is, in general, less than 1.3 dB up to 1.5 GHz, while the suppression band is from 2.65 GHz to 26.4 GHz with an attenuation level over 20 dB. Thus, the demonstrator shows a wide stopband with high suppression levels.

The simulated and measured S parameters of the prototype Filter C are shown in Fig. 6. It is found that the simulated 3 dB cut-off frequency is 2.22 GHz while the measured one is 2.035 GHz. The in-band insertion loss is about 1 dB up to 1.4 GHz. The filter also charac-terizes ultra-wideband suppression in which one can see to range from 2.95 GHz to over 26.5 GHz, the suppression levels are 20 dB except for a small peak near 14.5 GHz.

To further characterize the performance of the DGS filters, here a comprehensive index called figure-of-merit is introduced and studied. It is defined based on:

1) Suppression bandwidth (SBW) related to the 3 dB cut-off frequency of the measured filter, thus it is named normalized suppression bandwidth (NSBW) and given by

$$NSBW = \frac{SBW}{f_{c\_3dB}} \tag{14}$$

2) Suppression index (SI) that is related to the suppression level in the suppression band, for example, if the suppression level is referred to 20 dB, the SI is defined as 2.

3) Passband-to-stopband transition skirt (TS) that is referred to the 3 dB cut-off frequency and the concerned attenuation (CA) with its frequency (f_{ca}), given by

$$TS = \frac{CA(dB) - 3(dB)}{f_{ca}(GHz) - f_{c\_3dB}(GHz)} \tag{15}$$

4) Normalized size (NS) that is related to the layout footprint and the operation (cut-off) frequency of a filter, given by

$$NS = \frac{circuit\ size(length \times width)}{\lambda_g^2} \tag{16}$$

where λ_g is the guided wavelength referring to the 3dB cut-off frequency of the filter.

5) Layer index (LI) that is related to the PCB layers utilized since some types of DGS are of multi-layer architecture. For a DGS using one PCB layer, the LI is defined as 1.

Finally, the figure-of-merit (FoM) is defined as

$$FoM = \frac{NSBW \times SI \times TS}{NS \times LI} \tag{17}$$

It is noted that the FoM defined here can be more comprehensive by involving other parameters. For instance, the in-band return loss and/or insertion loss, etc, of such kind of filter.

To quantitatively study the FoM defined above, a comparison between some recently reported DGS LPFs is presented in Table 1. It is seen that the developed Filter B approaches the highest FoM of over 3.5×10^4 while it is over 3.1×10^4 for Filter C in this work. Both have high FoMs among the listed reports in Table 1. This means our design methodology in this contribution can characterize good comprehensive performance in terms of the filter's electric performance and geometric structure parameters.

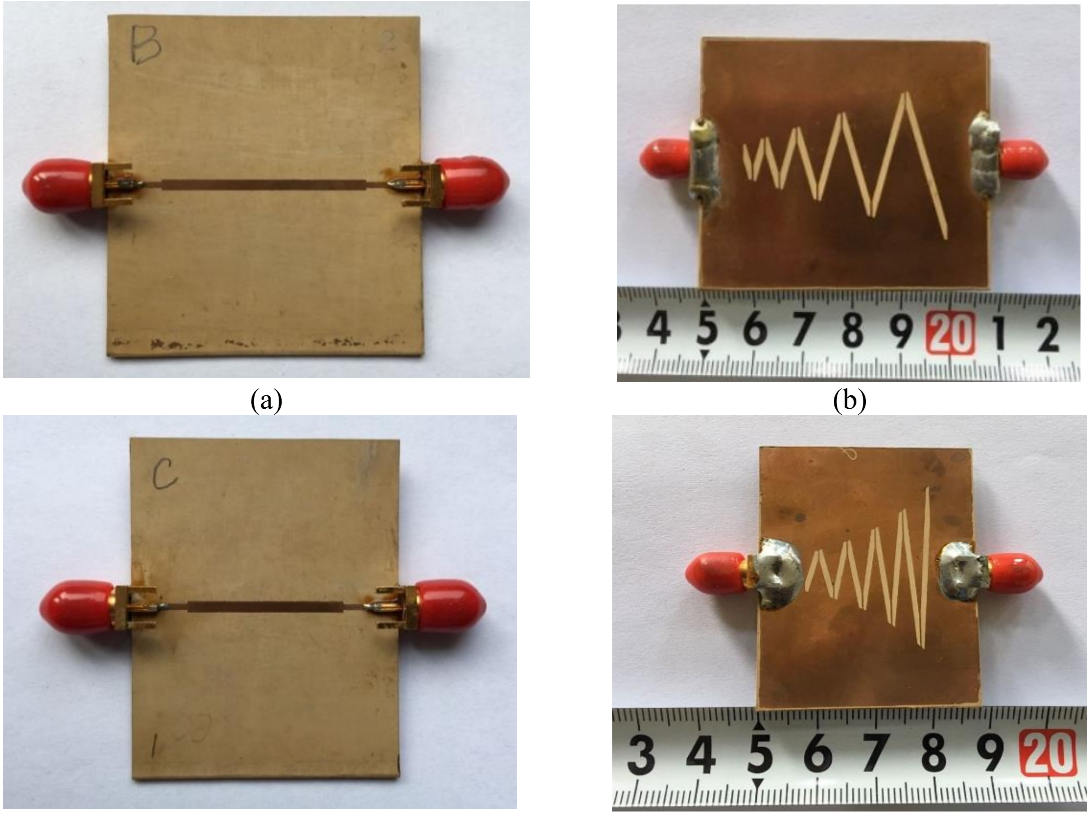

(a) (b)

(c) (d)

Fig. 4. Photographs of the developed prototype filters: (a) front side and (b) back side of Filter B, (c) front side and (d) back side of Filter C

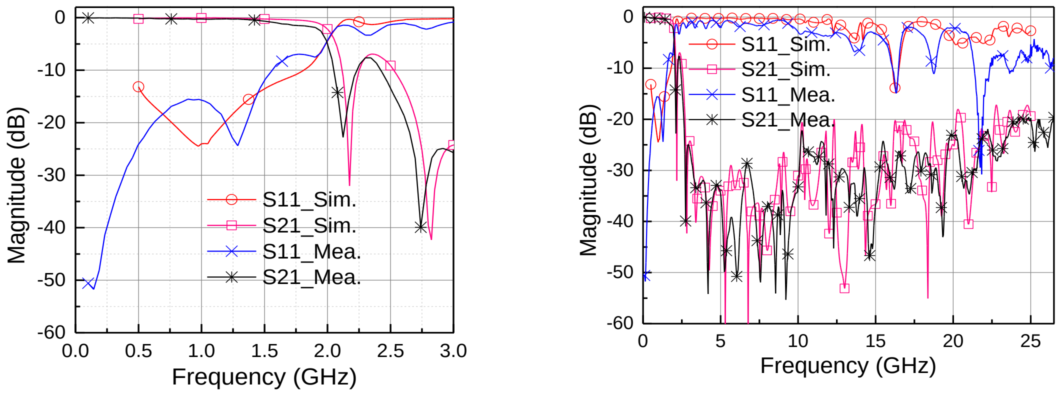

Fig. 5. Simulated and measured S-parameters of the prototype Filter B

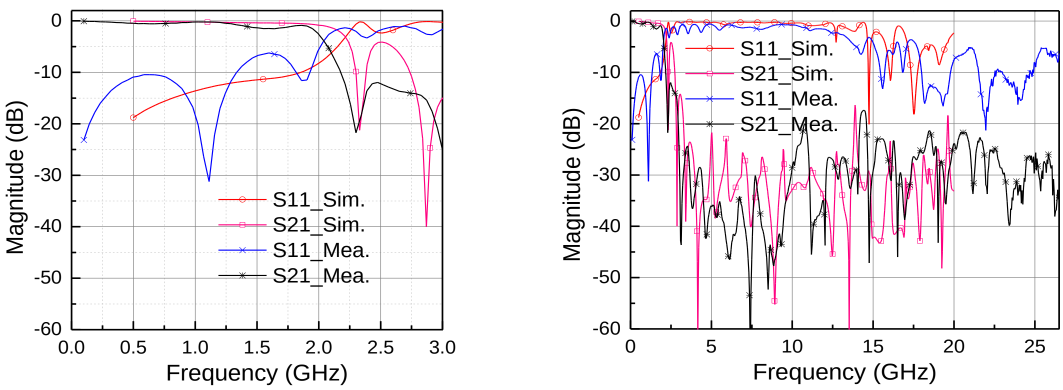

(a) (b)

Fig. 6. Simulated and measured S-parameters of the prototype Filter C

Table 1. Performance comparison of some reported DGS filters and our study in this work

Refs./ Years	f_{c_3dB} (GHz)	Suppr. range (GHz) & level	Trans. level & frequency	Layout footprint (mm^2)	Substrate parameters	LI	FoM ($\times 10^4$)
[3]/2017	2.0	2.2-6.3 @40 dB	40dB @2.2 GHz	36.8×24	$\varepsilon_r = 4.4$ $h = 0.8$ mm	1	~1.2
[4]/2019	2.2	2.7-12 @50 dB	40dB @2.65 GHz	100×2.6	$\varepsilon_r = 3.8$ $h = 0.254$ mm	3	~1.4
[5]/2020	3.62	4.45-20 @16.6 dB	30dB @4.64 GHz	14.85×18.4	$\varepsilon_r = 9.6$ $h = 0.8$ mm	1	~0.40
[7]/2020	1.96	2.61-26.5 @20 dB	40dB @2.74 GHz	40.653×29.546	$\varepsilon_r = 9.6$ $h = 0.8$ mm	1	~2.1
[11]/2020	2.11	2.27-20 @18 dB	20dB @2.57 GHz	15.5×12.7	$\varepsilon_r = 4.4$ $h = 0.8$ mm	1	~1.4
This work Filter B	1.965	2.65-26.4 @20 dB	40dB @2.75 GHz	30.307×31.17	$\varepsilon_r = 9.6$ $h = 0.8$ mm	1	~3.5
This work Filter C	2.035	2.95-26.5 @20 dB	40dB @3.085 GHz	22.35×31.524	$\varepsilon_r = 9.6$ $h = 0.8$ mm	1	~3.1

5. Conclusion

The slotline based zig-zag DGS for microstrip filter designs has been detailed in this study. By optimally determining a few (one or two) key parameters, DGS LPFs with good comprehensive performance can be achieved and based on this design methodology, the developed filters characterize sharp transition shirt, wide suppression band and high suppression levels as well as compact footprint. To further characterize this kind of filters, a comprehensive index called figure-of-merit (FoM) has been studied and defined, and high FoMs are demonstrated in this study for the proposed filters.

Acknowledgement

This work was supported in part by the Natural Science Foundation of China (NSFC) under grant no. 62271105.

References

[1] S.-S. Gao, J.-L. Li, R.-B. Chen, K. Song, Y.-S. Liu, J.-L. Xu and Y.-P. Li, 'Microwave lowpass filter with improved out-of-band performance based on tilted rectangular slots', *Journal of Electrical Engineering*, vol. 72, no.3, pp.213-216, June 2021.

[2] D. Zhang, K. Zhang, R. Dai, Q. Wu, T. Jiang, 'A compact lowpass filter based on spoof surface plasmon polaritons using defected ground structure', in *2019 IEEE Asia-Pacific Microwave Conference (APMC)*, Singapore, Dec. 10-13, 2019, vol. 1, no. Unit II, pp. 1434–1436.

[3] Z. L. Wen, Y.-N. Han, X.-Y. Sun, R. Tao, J.-N. Xia, X.-M. Chen, Y.-J. Chen, Z.-D. Chen, 'Design of miniaturized low-pass filter with improved Koch fractal DGS', in *IEEE International Symposium on Electromagnetic Compatibility*, Washington, DC, USA, Aug. 7-11, 2017, pp. 1–4, doi: 10.1109/EMC-B.2017.8260351.

[4] Q. Chen, K. Hu, S. Yuan, and C. Mei, 'A flexible microstrip lowpass filter design using asymmetric Pi-shaped DGS', *IEEE Access*, vol. 7, pp. 49999–50006, 2019, doi: 10.1109/ACCESS.2019.2910350.

[5] X.-O. Ou, R.-B. Chen, 'A hairpin DGS resonator for application to microstrip lowpass filters', *Journal of Electrical Engineering*, vol. 71, no. 2, pp.110-115, Apr. 2020.

[6] A. Ebrahimi, T. Baum, and K. Ghorbani, 'Differential bandpass filters based on dumbbell-shaped defected ground resonators', *IEEE Microwave and Wireless Components Letters*, vol. 28, no. 2, pp. 129–131, Feb. 2018, doi: 10.1109/LMWC.2017.2780765.

[7] R.-B. Chen, X.-O. Ou, J.-L. Li, B.A. Twumasi, 'Design of microwave lowpass filter based on log-periodic zig-zag DGS', *Journal of Electrical Engineering*, vol. 71, no. 6, pp. 428-432, Dec. 2020.

[8] S. Cao, Y. Han, H. Chen, and J. Li, 'An ultra-wide stop-band LPF using asymmetric Pi-shaped Koch fractal DGS', *IEEE Access*, vol. 5, pp. 27126–27131, 2017, doi: 10.1109/ACCESS.2017.2773577.

[9] X. K. Gao, H. M. Lee, and S. P. Gao, 'A robust parameter design of wide band DGS filter for common-mode noise mitigation in high-speed electronics', *IEEE Transactions on Electromagnetic Compatibility*, vol. 59, no. 6, pp. 1735–1740, June 2017, doi: 10.1109/TEMC.2017.2710202.

[10] B. Sahu, S. Singh, M. K. Meshram, and S. P. Singh, 'Simulation study of ultra-compact microstrip UWB bandpass filter with wide stopband using DGS based lowpass filter', in *IEEE MTT-S International Microwave and RF Conference, IMaRC*, Ahmedabad, India, Dec. 11-13, 2017, pp. 219–222, doi: 10.1109/IMaRC.2017.8449662.

[11] T.-K. Rekha, P. Abdulla, P.-M. Jasmine, and A.-A. Anu, "Compact microstrip lowpass filter with high harmonics suppression using defected structures", *AEU-International Journal of Electronics and Communications*, vol. 115, pp. 153032-1-10, 2020.

Jia-Lin Li received the M.S. degree from the University of Electronic Science and Technology of China (UESTC), Chengdu, China, in 2004, and the Ph.D. degree from the City University of Hong Kong in 2009, both in electronic engineering. From September 2005 to August 2006, he was a research associate with the Wireless Communication Research Center, City University of Hong Kong. From September 2009 to April 2021, he was with the School of Physics, UESTC, as a professor. Since May 2021, he has been with the School of Resources and Environment, UESTC. His research interests include microwave/millimeter-wave antennas and arrays, circuits and systems.

Baidenger Agyekum Twumasi was born at Nsawam in the Eastern Region of Ghana in September 1981. He obtained the HND in elect/electronic engineering from Ho Polytechnic (now Ho Technical University) in 2004, and the Master of Telecommunication Management from HAN University of Applied Sciences in Netherlands in 2011. He obtained the Doctor of Engineering in electronic science and technology from the University of Electronic Science and Technology of China in 2020. He is currently a senior lecturer in the department of Electrical/Electronic Engineering at Ho Technical University in Ghana. He is also a member of IEEE and a member of APS and MTTS societies. His research interests include antenna designs, electronic circuits for telecommunication applications, electromagnetic time reversal (EMTR) and its applications, wireless power transfer and its related circuits, microwave and millimeter-wave electronic circuits and systems design.

Rong-Bin Chen was born in Guangdong, China in January 1980. He received a BS Degree from Shantou University, Shantou, China, in 2003, and an M.S. Degree from Sun Yat-sen University, Guangzhou, China, in 2005. From July 2005 to June 2018, he was with the Jiangmen Branch of China Mobile Group Guangdong Co., Ltd., Jiangmen, China, where he served as a technique supporter for the maintenance, construction, and development of 2G/3G/4G/5G wireless/mobile networks. Since June 2018, he has been with the Department of Electronic and Information Technology, Jiangmen Polytechnic, Jiangmen, China. His research interests include wireless communication technology and the Internet of Things.

Shan-Shan Gao was born in Sichuan, China. She received the M.Sc. and Ph.D. Degree from the University of Electronic Science and Technology of China (UESTC), Chengdu, China, in 2008 and 2012, both in electronic engineering. Since July 2013, she has been with the School of Electronic Information and Electrical Engineering, Chengdu University, Chengdu, China, where she is currently a professor. Her research interests include design and realization of microwave passive devices and circuits.